

Surface anisotropy of a Fe_3O_4 nanoparticle: A simulation approach

J. Mazo-Zuluaga^{a,*}, J. Restrepo^a, J. Mejía-López^b

^aGrupo de Estado Sólido, Grupo de Física y Astrofísica Computacional, Universidad de Antioquia, A.A. 1226 Medellín, Colombia

^bFacultad de Física, Pontificia Universidad Católica, Avenida Vicuña Mackenna 4860, Santiago, Chile

Abstract

On the basis of a three-dimensional classical Heisenberg model with nearest magnetic neighbor interactions, and using a Monte Carlo–Metropolis dynamics, we study the magnetic behavior of a 5 nm diameter magnetite nanoparticle as a function of temperature. The nanoparticle is built by taken into account the inverse spinel structure of a stoichiometric magnetite, the valence of the iron ions (Fe_A^{3+} , Fe_B^{3+} , Fe_B^{2+} where A and B stand for tetrahedral and octahedral sites, respectively) as well as the different involved coordination numbers and superexchange integrals. The employed Hamiltonian includes coupling interactions between Fe ions through the integrals J_{AA} , J_{AB} and J_{BB} , a Néel's surface anisotropy term applied to surface ions, and cubic magnetocrystalline anisotropy for those ions belonging to the core of the nanoparticle. Results reveal a strong influence of surface anisotropy, depending on its sign and magnitude, upon the total magnetization at low temperatures. Such results, which are summarized in a proposal of phase diagram, reveal the onset of spin structures different from a single-domain state. Differences in the thermal behavior respect to a bulk magnetite are also addressed and discussed. © 2007 Elsevier B.V. All rights reserved.

Keyword: Magnetite; Nanoparticles; Monte Carlo; Surface anisotropy

1. Introduction

Magnetite is a well-known material due to its extensive use and different applications. It has been used in traditional recording media, and has played an important role in the field of spintronics [1]. It is also well known that magnetic properties exhibited by nanoparticles are different from those found under bulk conditions, and they are strongly dependent upon finite size effects. Such effects include changes in the average coordination number and the presence of uncompensated spins due to the breaking of symmetry at the boundaries. Other features like roughness, relaxation and structural disorder on the surface increase the complexity of these systems [2–4]. Moreover, the influence of surface anisotropy upon such properties is still a subject of controversy. The aim of this work is to investigate the magnetic properties of a single- Fe_3O_4 magnetite spherical-shaped nanoparticle by using the Monte Carlo–Metropolis method. The inverse spinel structure has been simulated with free boundary conditions

to take into account surface effects for a 5 nm diameter nanoparticle. The different superexchange integrals involving tetrahedral and octahedral sites and the real coordination numbers have been also considered.

2. Model and simulation details

Magnetite is a ferrimagnetic compound below around 859 K [5]. It is characterized for having Fe^{3+} ions (with spin $S = 5/2$) and Fe^{2+} ions ($S = 2$) distributed in two sublattices with different O^{2-} coordination. In the model, we have considered the inverse spinel structure with space group $\text{Fd}3\text{m}$ and 32 oxygen and 24 iron ions per unit cell. This structure consists of eight tetrahedral positions (or A-sublattice) occupied by Fe^{3+} ions and 16 octahedral sites (B-sublattice) having eight Fe^{2+} and eight Fe^{3+} ions randomly distributed. This random distribution has been implemented in order to consider the mixed valence $\text{Fe}^{2.5+}$ state resulting from the electron hopping mechanism between Fe_B^{3+} and Fe_B^{2+} as it has been observed via Mössbauer experiments [5]. Here we focus our attention on the properties of a 5 nm diameter magnetite nanoparticle by implementing free boundary conditions.

*Corresponding author. Tel.: +57 4 2105630; fax: +57 4 2105666.
E-mail address: jomazo@fisica.udea.edu.co (J. Mazo-Zuluaga).

The employed model is based on a three-dimensional classical Heisenberg Hamiltonian with magnetocrystalline anisotropy, Néel's surface anisotropy and interactions within the first magnetic coordination shell. Magnetic ions Fe_A^{3+} , Fe_B^{3+} , and Fe_B^{2+} are represented by classical Heisenberg spins, whereas oxygen ions are considered as non magnetic. Spins interact via antiferromagnetic superexchange interactions with nearest magnetic neighbors when considering A–A or A–B bonds; whereas ferromagnetic couplings are considered for B–B, interactions. The Hamiltonian of our system can be written as follows:

$$H = -2 \sum_{\langle ij \rangle} J_{ij} \vec{S}_i \cdot \vec{S}_j - K_S \sum_k (\vec{S}_k \cdot \hat{n}_k)^2 - K_V \sum_i (S_{x,i}^2 S_{y,i}^2 + S_{y,i}^2 S_{z,i}^2 + S_{x,i}^2 S_{z,i}^2). \quad (1)$$

The first sum runs over nearest magnetic neighbors with the following coordination numbers depending on the crystallographic site: $z_{AA} = 4$, $z_{BB} = 6$, $z_{AB} = 12$ and $z_{BA} = 6$. The second term accounts for the single-ion site surface anisotropy and the unit vector on the surface at each i th position with vector \vec{P}_i , is computed according to [6]:

$$\hat{n}_i = \sum (\vec{P}_i - \vec{P}_j) / \left| \sum (\vec{P}_i - \vec{P}_j) \right|, \quad (2)$$

where the sum runs over j index, representing the magnetic neighbors of the i th ion. The third term in Eq. (1) gives the core cubic magnetocrystalline anisotropy where K_V ($= 1.35 \times 10^4 \text{ J/m}^3$) is the bulk anisotropy constant [7].

Numerical values of the employed integrals were taken from the first principles study of superexchange integrals for magnetite in the nearest-neighbor approximation by Uhl and Siberchicot [8]. Such values are $J_{AA} = -0.11 \text{ meV}$, $J_{AB} = J_{BA} = -2.92 \text{ meV}$ and $J_{BB} = +0.63 \text{ meV}$ and they reproduce the Curie temperature of stoichiometric magnetite (859 K). In our simulation, we have employed a single-spin movement Metropolis Monte Carlo algorithm for computing equilibrium thermodynamic properties. For the bulk system, periodic boundary conditions and a linear system size $L = 10$, with a total number of magnetic ions $N = 24 \times L^3$ ($= 24000$ ions), were considered. Additionally, a closely spherical nanoparticle with free boundary conditions having 2731 Fe ions and a diameter of 5 nm was also considered. Relaxation effects of the surface ions are not taken into account in the present work. This feature is currently under progress to go further in our study. On the other hand, even though the elastic energy is usually greater than the magnetic one, such contribution enters as a constant in the internal energy as far as the ions positions are considered fixed, and therefore it can be neglected in the framework of a purely magnetic Hamiltonian.

Simulated annealing from well above the Curie temperature was carried out by starting from a random spin configuration corresponding to infinite temperature in

order to obtain the temperature dependence of the magnetization. Up to three different configurations and around 1.4×10^4 Monte Carlo steps per spin (mcs) were considered in order to compute equilibrium averages. The computed basic equilibrium thermodynamic quantities were the total energy, the magnetization per spin, the magnetic susceptibility and the specific heat. Magnetic contributions to the total magnetization per magnetic site arising from A and B sites were also analyzed separately. This fact constitutes one of the advantages of the Monte Carlo simulation compared to experimental bulk magnetic measurements. Finally, the ratio K_S/K_V was taken to range between -10^6 and 10^6 . Such a wide range allows determining the magnetic stability of the involved magnetic structures and modeling different scenarios regarding the matrix which nanoparticles can be embedded in [9–11].

3. Results and discussion

Fig. 1 shows the temperature dependence of the modulus of the magnetization per spin, including the A and B contributions, under bulk conditions. The obtained total magnetization, lying below these contributions, reveals effectively the occurrence of ferrimagnetic order, i.e., antiparallel alignment between A and B sublattices. Magnetic susceptibility is also shown in this figure, indicating the bulk critical temperature at $T_C = 859 \pm 3 \text{ K}$ as is expected.

As far as the nanoparticle is concerned, the temperature dependence of the computed quantities is qualitatively similar to that shown in Fig. 1, but quantitatively three differences respect to the behavior of the bulk magnetite are evidenced. First, results reveal a reduction of the Curie temperature T_C as compared to that obtained for a bulk magnetite when using periodic boundary conditions. This feature is evident from Figs. 2 and 3, where the

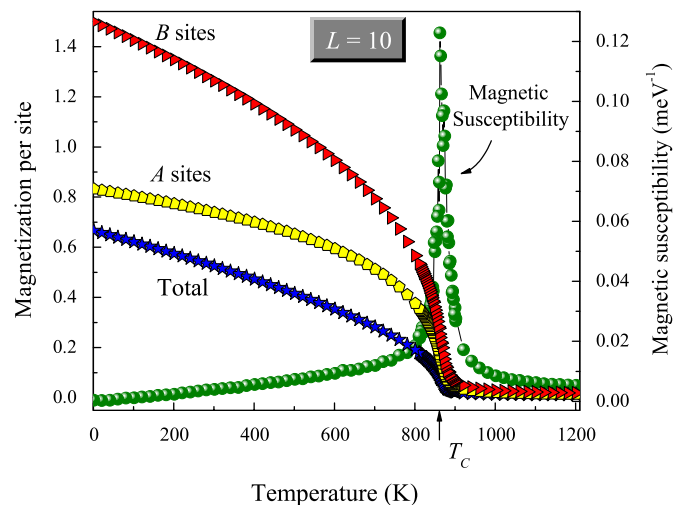


Fig. 1. Temperature dependence of the magnetization and magnetic susceptibility for magnetite. Critical temperature is estimated from the position at which the maximum of the susceptibility occurs.

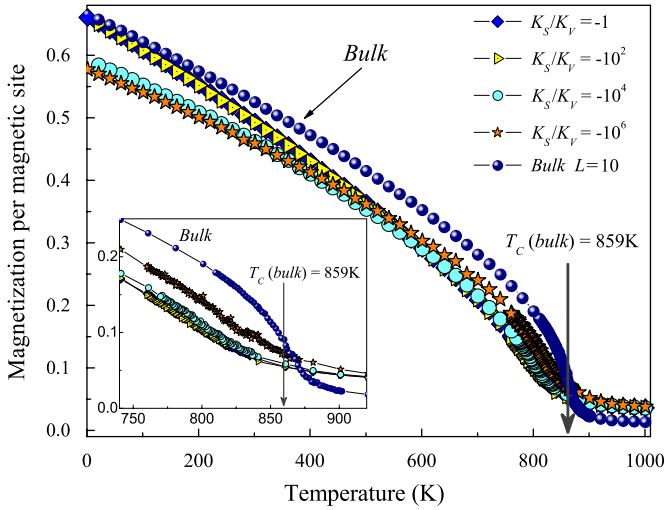


Fig. 2. Temperature dependence of the magnetization for some selected K_S/K_V negative values. For comparison the bulk magnetization is also included. Inset shows a zoom of the critical region.

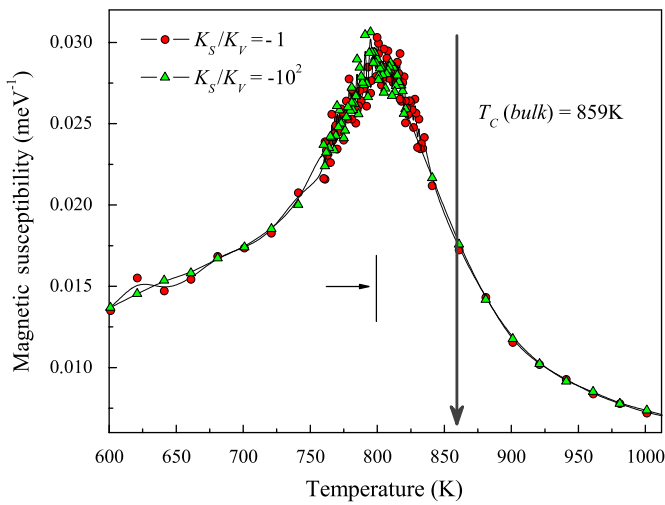


Fig. 3. Temperature dependence of the magnetic susceptibility for some selected K_S/K_V negative values. For comparison, the bulk T_C value is shown.

thermal dependence of magnetization and magnetic susceptibility are shown for some selected values of K_S/K_V . Such a reduction in T_C , which is of the order of 60 K, is attributed to the decrease of the average coordination number and consequently to the smaller density of magnetic bonds. This fact is in turn a consequence of symmetry breaking occurring at the surface of the nanoparticle.

Second, a smoother tail at around T_C , as well as the rounded peaks of the susceptibility and the specific heat (not shown), are the typical signature of a finite size effect.

Finally, concerning the low-temperature behavior, it must be stressed that the resulting magnetic structure depends upon the surface anisotropy and consequently the magnetization becomes affected. Magnetizations at the low-temperature region, compared to that obtained in

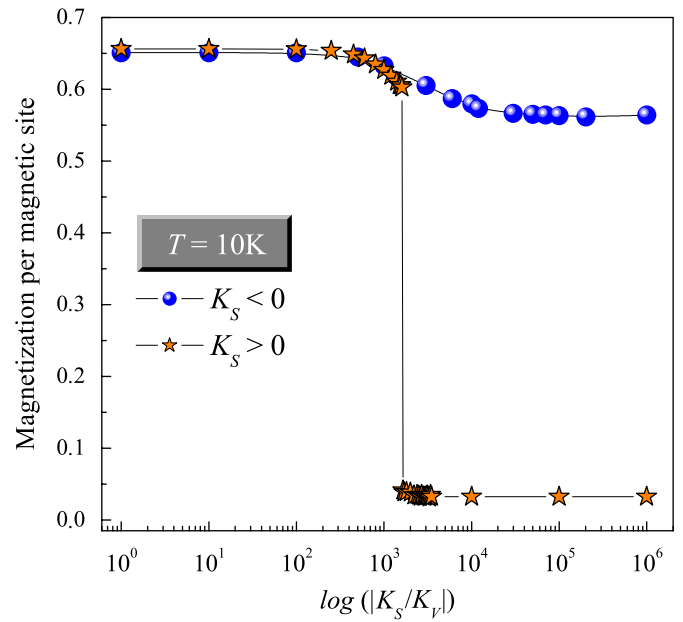


Fig. 4. Magnetization computed at $T = 10$ K, as a function of the K_S/K_V magnitude.

Fig. 1 for the bulk case, exhibit a marked reduction which becomes greater as K_S/K_V increases. As shown in Fig. 4, results exhibit a non-symmetric behavior depending on the sign of K_S . More concretely, as K_S becomes more positive the magnetization diminishes more rapidly than that obtained for negative K_S values. This means that the mechanism by which the system undergoes the ferrimagnetic to paramagnetic transition depends on the magnitude of the surface anisotropy. For positive values, as K_S increases, those spins belonging to the surface tend to be oriented in a closely radial fashion. Such information is in turn propagated through the core via superexchange couplings, giving rise finally to the onset of a spike-type configuration when the ratio K_S/K_V becomes as higher as 10^3 (see Fig. 4). Contrary to this, as K_S becomes more negative, the magnetic moments on the surface are oriented in a tangential way. Both situations are accompanied by a reduction of the magnetization. These features reveal a clear deviation from a single-domain phenomenology. It is also important to mention that the antiparallel alignment between moments of the A and B sublattices is not affected by K_S , preserving in this way the ferrimagnetic order.

4. Conclusions

From our results, a remarkable reduction of T_C for the nanoparticle respect to the bulk case is concluded. This reduction is attributable to symmetry breaking at the surface and consequently to a lower density of magnetic bonds. Results allow concluding remarkable differences in the magnetic behavior depending on the sign and magnitude of the K_S/K_V ratio. Finally, for low K_S/K_V ratios, the nanoparticle exhibits a close single-domain state, different to that observed as K_S/K_V increases.

Acknowledgments

This work was supported by different projects: COLCIENCIAS 1115-05-17603 and CENM 043-2005; FONDECYT Grant 1050066; collaboration project COLCIENCIAS-CONICYT Colombia-Chile Folio 2005-206; and Universidad de Antioquia: SIU-24-1-28 GES and IN1247CE-CODIGICM. J. Mazo-Zuluaga thanks to COLCIENCIAS, “Vicerrectoría de Investigación UdeA” and “Vicerrectoría de Docencia UdeA” for financial support.

References

- [1] A. Gupta, J.Z. Sun, *J. Magn. Magn. Mater.* 200 (1999) 24.
- [2] R.H. Kodama, A.E. Berkowitz, E.J. McNiff Jr., S. Foner, *Phys. Rev. Lett.* 77 (1996) 394.
- [3] R.H. Kodama, A.E. Berkowitz, *Phys. Rev. B* 59 (1999) 6321.
- [4] J. Restrepo, Y. Labaye, L. Berger, J.M. Greneche, *J. Magn. Magn. Mater.* 272–276 (2004) 681.
- [5] R.M. Cornell, U. Schwertmann, in: *The Iron Oxides* VCH mbH, Weinheim, Germany, 1996.
- [6] R.H. Kodama, A.E. Berkowitz, *Phys. Rev. B* 59 (1999) 6321.
- [7] G.F. Goya, T.S. Berquó, F.C. Fonseca, M.P. Morales, *J. Appl. Phys.* 94 (2003) 3520.
- [8] M. Uhl, B. Siberchicot, *J. Phys.: Condens. Matter* 7 (1995) 4227.
- [9] H. Kachkachi, E. Bonet, *Phys. Rev. B* 73 (2006) 224402.
- [10] D.A. Garanin, H. Kachkachi, *Phys. Rev. Lett.* 90 (2003) 065504.
- [11] O. Iglesias, A. Labarta, *Physica B* 343 (2006) 286.